UK Structure Site Report: Boddam Fault, Peterhead Granite

T L STEPHENS, T ARMITAGE, M SCHILTZ*, R HASLAM

BGS REPORT NUMBER: OR/25/064

British Geological Survey

* TownRock Energy

Abstract
Understanding the architecture and connectivity of faults and fractures in granitic intrusions is critical for understanding fluid-flow in deep geothermal systems (DSGs). The Boddam fault zone cross-cuts the Peterhead granite, and provides an excellent analogue for the subsurface expression of fault and fracture zones in granitic bodies. The fault system comprises offset NNE-SSW striking fault segments inferred to link at a relay zone, at Boddam Castle, via NE-SW sinistral and NW-SE dextral strike-slip faults. A series of N-S high-angle reverse faults also occur, but their relationship to the fault zone is uncertain. The relay zone displays a high fault and fracture density and connectivity which could contribute to enhanced fluid flow in the system. The work suggests that fault relay zones could be considered as higher-permeability targets for geothermal exploration.

Acknowledgements
This work was undertaken as part of the British Geological Survey's National Geoscience UK Structure programme. The work was undertaken in collaboration with TownRock Energy as a knowledge exchange activity.

Mike Schiltz (TownRock Energy) is thanked for providing valuable observations and discussions in the field along with collection of fracture data.

Tim Kearsey (BGS) and Jon Ford (BGS) are thanked for review of the document.

Statement of Intent

The data pack is intended as a resource that provides an overview of fault structure and fault network architecture in Granitic lithologies, using an example from Peterhead, Aberdeenshire. The work highlights the complexity of major faults that is not resolvable on 1:50 000 and 1:10 000 scale geological maps, where faults are expressed as a single line. The data pack can be used as an analogue for understanding potential fault networks in the subsurface in similar intrusions. The data pack focusses on horizontal and vertical outcrops along coastal cliff sections.

Bibliographical reference
STEPHENS, T. L., ARMITAGE, T., SCHILTZ, M., HASLAM, R. 2026. UK Structure Site Report: Boddam Fault, Peterhead Granite. *British Geological Survey Open Report*, OR/25/064. 19pp.

BGS Report No. OR/25/064

BGS Project Code: NEE7165S

Front cover photo: View north of the Boddam Fault zone at Boddam Castle, Peterhead. See also slide 8. BGS image P1080439 © UKRI 2024.

Report Issued: 03 / 03 / 2026

This report uses Cardinal Coordinate notation when referring to dip directions or trends of features, e.g.:

- **N** north
- **NE** north-east
- **NNE** north-north-east
- **N-S** north-south

Summary

Geothermal energy provides a constant and reliable heat source and could play an important role in contributing towards UK decarbonisation and net zero targets. Deep Geothermal Systems (DGS) occur at depths 500 - 5000 m (current max economic drilling depth). Prospective DGS's have been identified across the UK in sedimentary basins and granitic plutons, including the Scottish Caledonian Late Silurian-Early Devonian 'Newer Granite' suite. Since granites are typically tight, geothermal production relies on fluid-flow through open fault and fracture systems. Characterising fault zone architecture in granite bodies, particularly from surface analogues, is of critical importance to understanding DGS permeability and geothermal resource potential in the subsurface.

The Boddam Fault Zone cuts the Peterhead Granite and is well exposed along the Peterhead coastline. The fault system strikes NNE-SSW, with a minimum inferred length of 1.8 km, and comprises offset NNE-SSW striking fault segments inferred to link via ENE-WSW sinistral and NW-SE dextral strike-slip faults. A series of N-S high-angle reverse faults also occur, but their relationship to the fault zone is uncertain. The major fault segment comprises a ~15 m wide zone; within this zone lensoidal blocks of relatively intact rock are separated by bounding faults ranging from 10s of cm to 10s of metres length. Fracture intensity varies across the site area, with most intense fracturing recorded within the fault zone. The study area is inferred to represent a relay zone between the two major fault segments. High fault and fracture intensity in this zone could contribute to enhanced fluid flow, suggesting fault relay zones should be considered as targets for geothermal exploration.

This datapack provides an overview of the Boddam Fault, characterising the associated deformation observed within the Peterhead Granite, showcasing patterns of brittle deformation with granites and presents a conceptual structural model for the Boddam coastline. Within this, the geothermal prospectivity of the granite is assessed at a high level, with fault zone deformation and regional fracture networks identified that may continue in the subsurface and enhance permeability at depth.

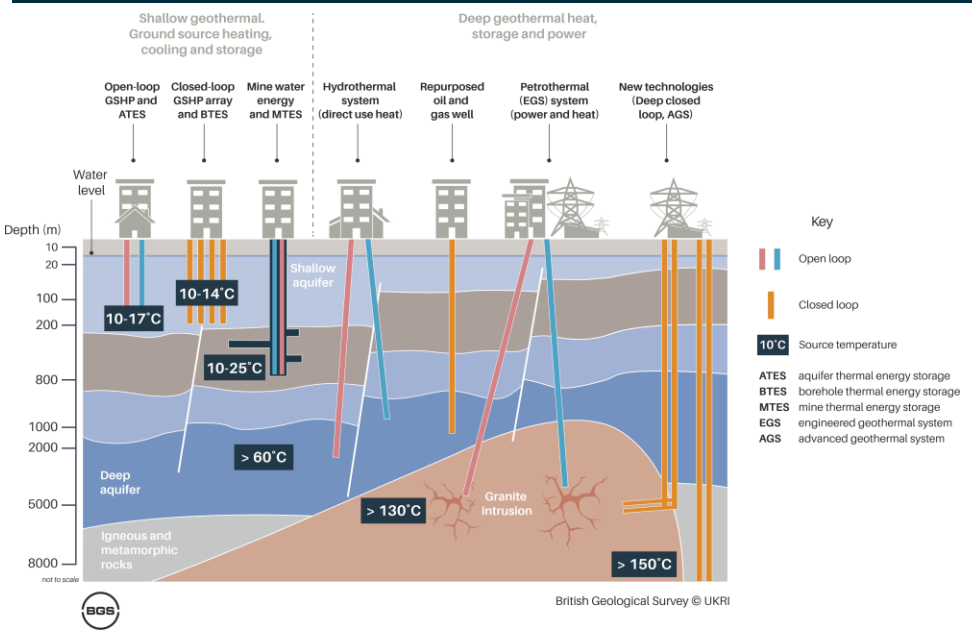

Figure 1. Schematic geological diagram outlining potential geothermal technologies and highlighting the potential for deep geothermal systems including granitic intrusions and deep metamorphic basement. British Geological Survey © UKRI.

Geological Context

Large, relatively undeformed granitoid bodies are commonly found throughout the Northern Highlands, Grampian, Midland Valley, Southern Uplands and Leinster-Lakesman terranes of the British Caleodnides. These are termed late Caledonian or the ‘Newer Granite’ suite to distinguish relatively undeformed Silurian–Devonian intrusive rocks from the ‘Older Granite’ suite of mainly foliated plutons that were emplaced prior to, and during the early stages of, the Caledonian orogeny (Lambert and McKerrow, 1976; Oliver et al., 2008). The emplacement ages of late Caledonian plutonic rocks are constrained between *c*. 437 and 370 Ma, with the majority emplaced between *c*. 425 and 415 Ma (Archibald et al., 2022 and references therein). Although the Peterhead Pluton has widely been regarded as a member of the ‘Newer Granite’ suite, this would appear to be incorrect based on a new high-precision U–Pb zircon age of c. 471 Ma obtained from a sample of the typical coarse granite collected in the nearby Stirlinghill Quarry (S. Tapster, S. Parry pers. comm. 2025).

In the Northern Highland and Grampian terranes, Caledonian thrusting was followed by emplacement of steep-sided plutons that are thought to have commonly exploited steep, strike-slip shear zones and faults. Here, magmatism is thought to have resulted from slab break-off following the closure of the Iapetus Ocean (Atherton and Ghani, 2002). Following slab break-off, rapid exhumation of the Caledondies unroofed late Caledonian granites, beginning erosion and sedimentation as found in the Lower Devonian Crawton Group in the Midland Valley terrane (Haughton and Halliday, 1991).

Due to their relatively late emplacement post-dating the main phases of Caledonian metamorphism, Newer Granites do not typically hold ductile structures. Instead, brittle fractures and faults are found, perhaps associated with cooling and post-Devonian regional tectonic events (e.g., Kicks et al., 2013; Holdsworth et al., 2015).

The Peterhead Granite is hosted within semi-pelites and psammites of the Dalradian Supergroup and intrudes the sillimanite core of Barrovian metamorphism in NE Scotland. E-W trending dykes, of the North Britain Late Carboniferous tholeiitic suite, cross-cut the granite. Dyke compositions include dolerite, and quartz microgabbro (c.f. dolerite).

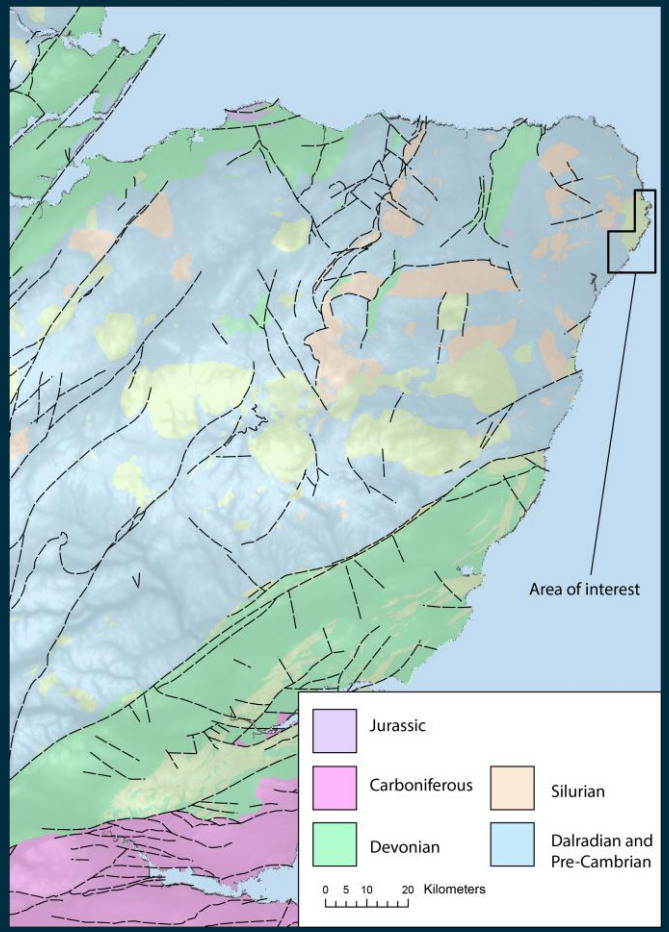

Figure 2. Overview geological map of Scotland showing the location of the Peterhead site area. The map is coloured by geological Period, and the Newer Granite Suite are coloured yellow. The map contains a hillshade produced from NEXTMap-50 DTM Data (NEXTMap Britain elevation data from Intermap Technologies). British Geological Survey © UKRI 2026.

Site Description

The Peterhead Granite is exposed along a series of cliff faces (c. 10 – 30 m high) from Cruden Bay to Peterhead which have mixed accessibility. Throughout the coastline are inlets and gorges orientated c. N-S and E-W, likely exploiting lithological contacts with the tholeiitic dyke suite and structural weaknesses.

A walk-over survey along the Peterhead coastline identified a NNE-SSW trending fault system that is best exposed on the coastline near the village of Boddam and extends from Boddam Lighthouse southwards to Dundonnie (Figure 2). This fault has not been previously mapped and is named here the 'Boddam Fault'.

The fault system strikes NNE-SSW and comprises a series of offset NNE-SSW striking fault segments inferred to link via ENE-WSW and NW-SE strike-slip faults. A series of N-S high-angle reverse faults also occur, but their relationship to the fault zone is uncertain.

At Boddam Castle the major fault segment comprises a ~15 m wide zone; within this zone lensoidal blocks of relatively intact rock are separated by bounding faults ranging from 10s of cm to 10s of metres length. Fracture intensity varies across the site area, with most intense fracturing recorded within the fault zone.

The fault zone is also partially exposed at Boddam Lighthouse at low tide, where the fault forms the boundary between a porphyritic microgranite intrusive body and the Peterhead Granite.

The following slides provide more detail of the fault and fracture systems in these key areas.

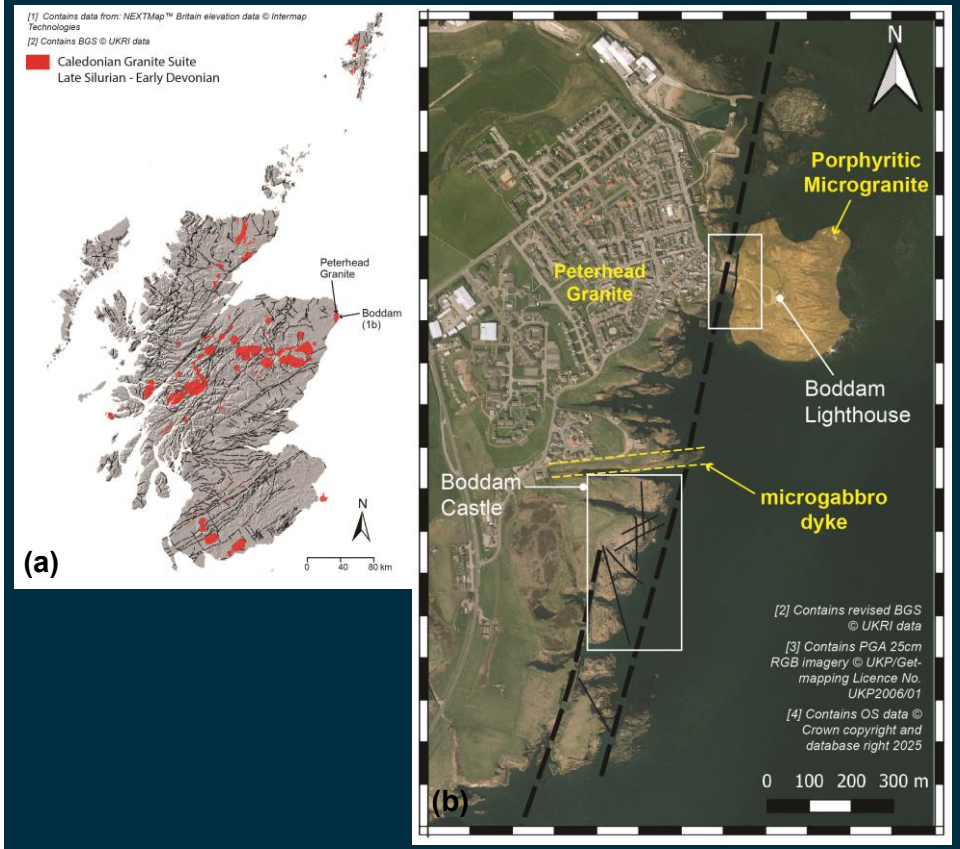

Figure 3. (a) Terrane map showing the location of the Caledonian Late Silurian – Early Devonian Granite suite, and Peterhead. (b) The Boddam study area, white rectangles show study areas at Boddam Castle (Slide 7) and Boddam Lighthouse (slide12).

Peterhead Granite

The Peterhead Granite is a mostly homogenous coarsely crystalline granite, predominantly comprising quartz (2-10 mm, ~30%), plagioclase feldspar (2-10 mm, ~20%), and pink k-feldspar (2-10 mm, ~50%) (Figure 4a). Micas were rare in the study area, but variably chloritized biotite is a common constituent of the Peterhead Granite more generally. The granite has a pink colour in outcrop, and weathers to a pale grey.

The Boddam Lighthouse Microgranite is porphyritic with phenocrysts of quartz (~1-2 mm) in a finely crystalline groundmass comprising <1 mm crystals of quartz, plagioclase feldspar, and k-feldspar (Figure 4b). The microgranite becomes aphanitic towards its margin and changes from a pink-orange colour to a purple-red colour, inferred to represent a chilled margin.

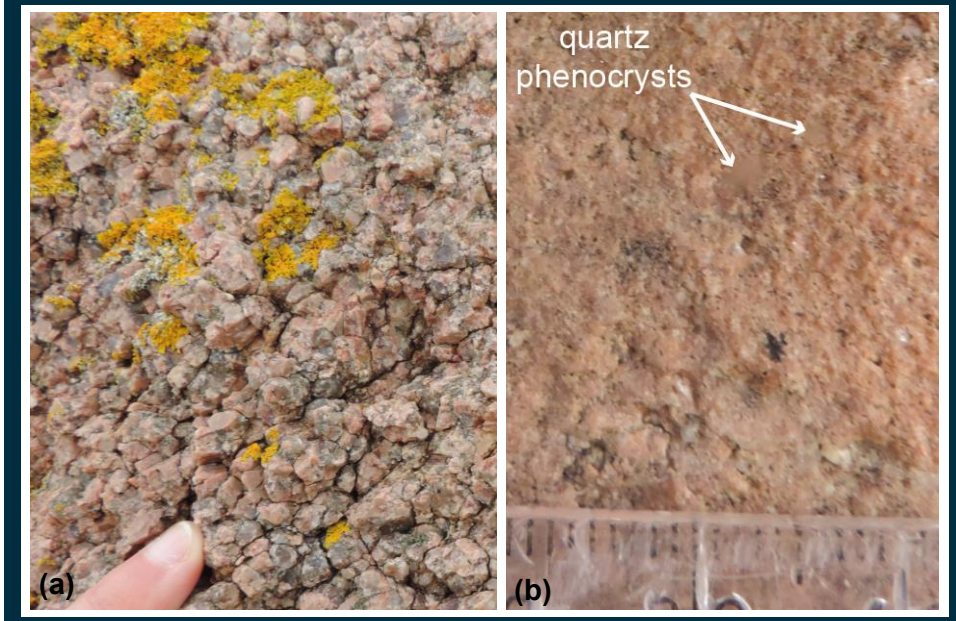

Figure 4. Examples of: (a) Peterhead coarse granite, and (b) Boddam Lighthouse Microgranite. BGS image P1080122 and P1080439 © UKRI 2024.

Boddam Castle

FAULT STRUCTURE

At Boddam Castle the western bounding fault zone trends N-S and comprises an c.15 m wide zone of fault-bound blocks (Figure 5). The bounding fault dips steeply to the west (Figure 6). To the East of the bounding fault, additional major fault sets include ENE-WSW sinistral faults and NW-SE dextral faults, which form fault-fracture corridors, and N-S striking reverse-oblique faults (Figures 5 and 6).

The ENE-WSW sinistral and NW-SE dextral faults may represent R' and P Reidel shears within an overall dextral relay zone (Figure 5). The reverse faults are miss-matched relative to this system and may represent reactivation of earlier structures or a later phase of deformation.

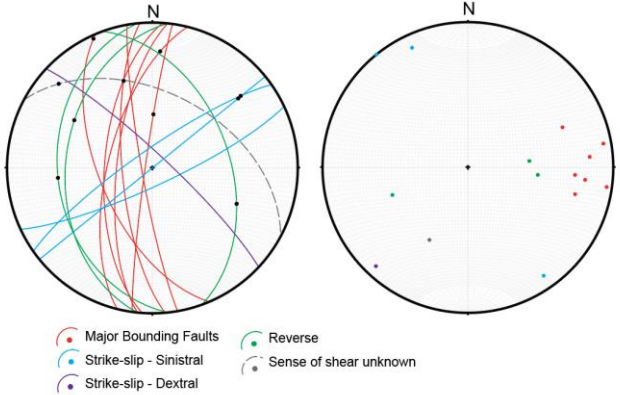

Figure 6. Lower hemisphere equal area stereonets to show major faults in the Boddam Fault Zone as planes, and poles to planes. Slickenlines plotted as rake on planes. British Geological Survey © UKRI 2026.

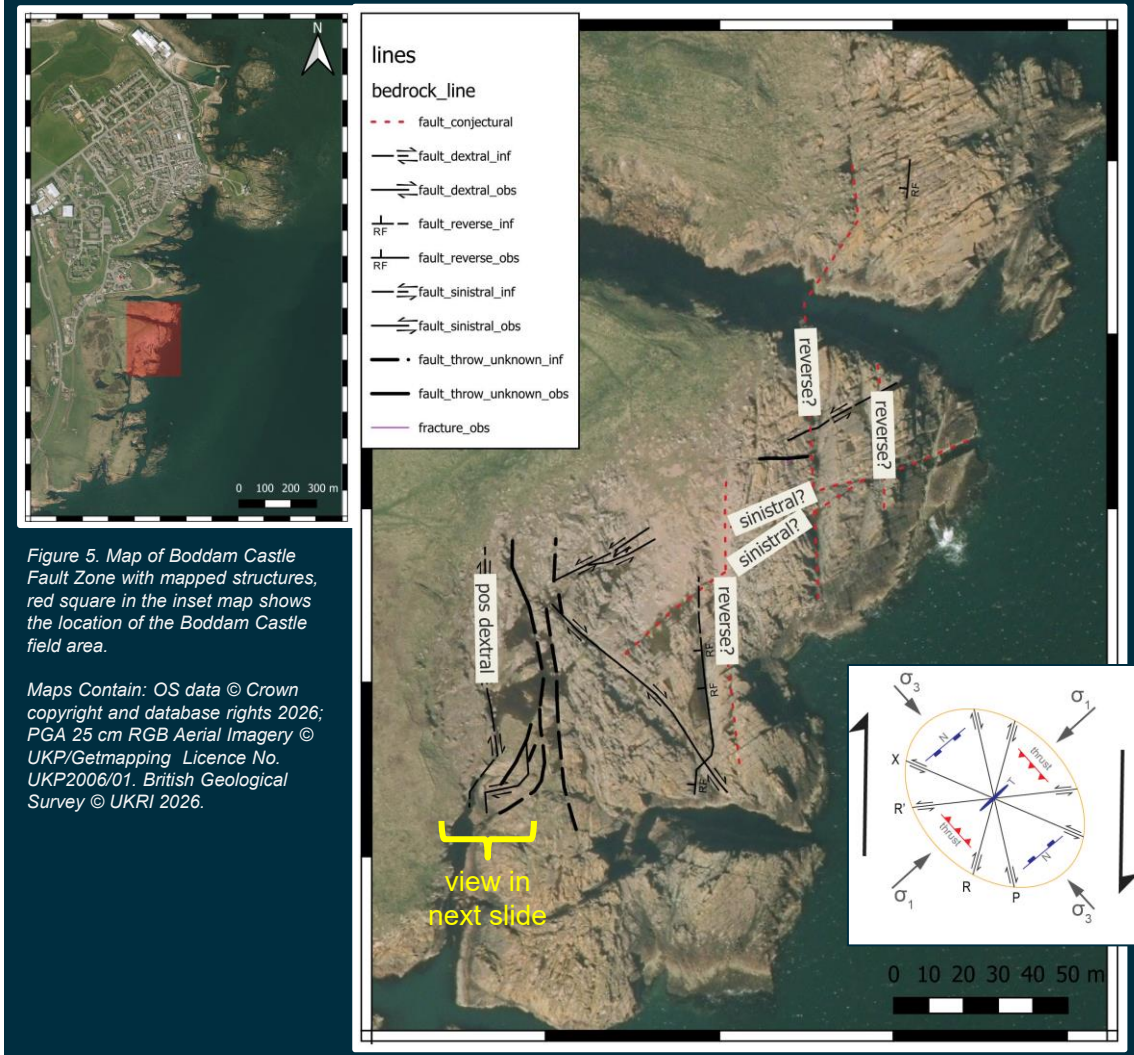

Figure 5. Map of Boddam Castle Fault Zone with mapped structures, red square in the inset map shows the location of the Boddam Castle field area.

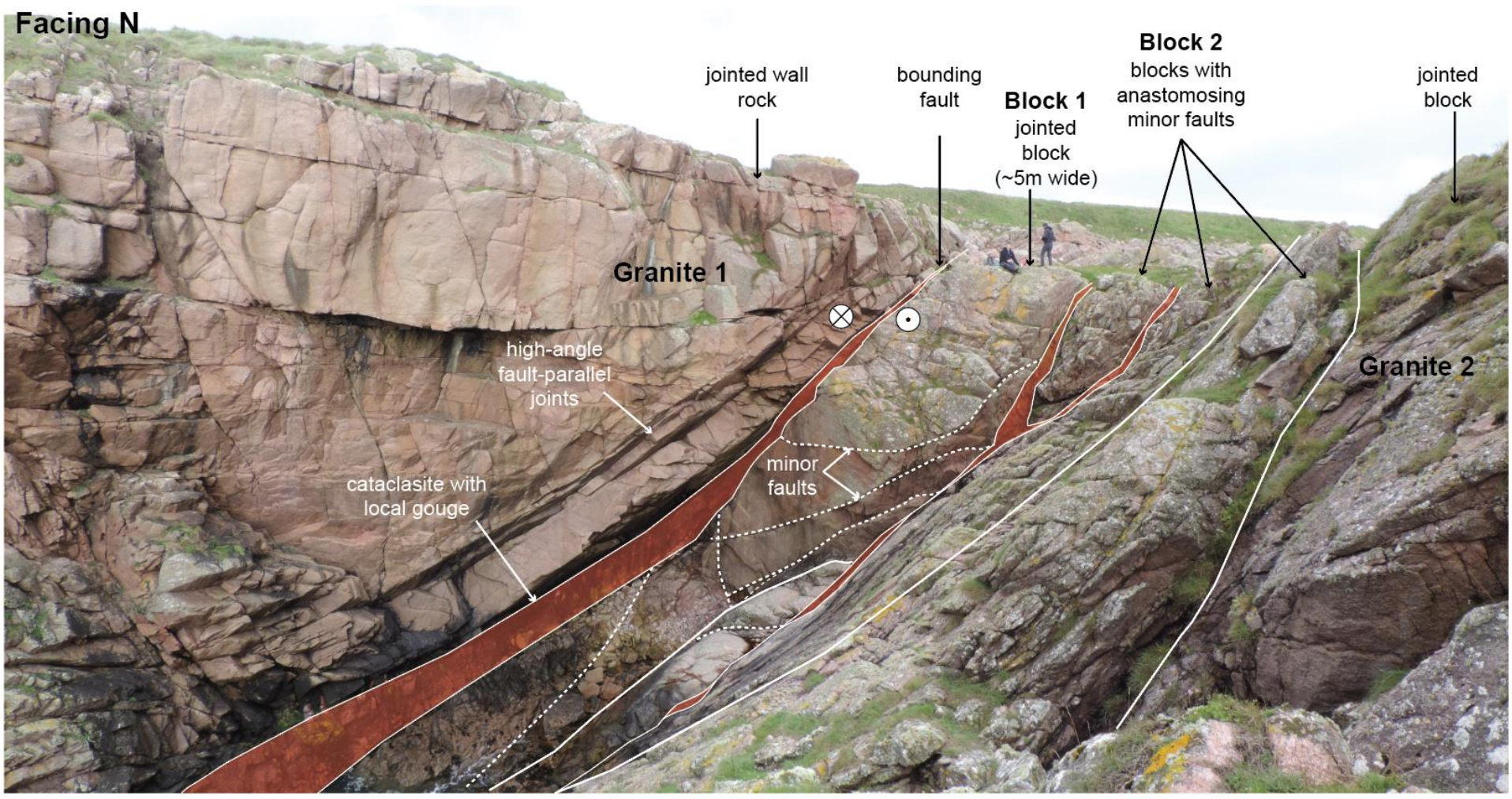

Figure 7. Annotated photograph of a cliff-section through the Boddam Fault Zone, at Boddam Castle. The area is divided into blocks which correlate to different fracture intensities. BGS image P1080439 © UKRI 2024.

Boddam Castle

FAULT ZONE ARCHITECTURE & FAULT ROCK

In the Boddam Castle area the major bounding fault has local meter-wide zones of breccia which comprise blocks of intact granite surrounded by protobreccia and clay gouge (Figure 8a,c,d). Anastomosing fault networks bound sinuous lensoids of relatively intact granite (Figure 8b). These faults comprise 1-2 cm wide bands of cataclasite which are preferentially eroded. Adjacent to the main fault, is an c.60 cm zone of mm-spaced fault-parallel fractures (Figure 9).

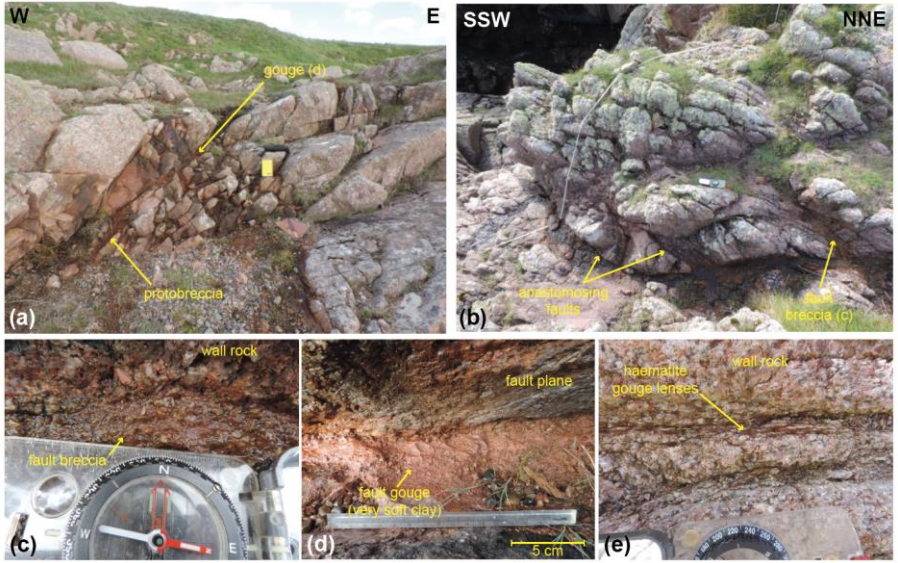

Figure 8. Examples of different fault rocks observed in the Boddam Fault Zone. BGS images P1080344, P1080323, P1080327, P1080343 © UKRI 2024.

The ENE-WSW and NW-SE trending fault-fracture corridors vary from 0.2 – 1 m in width and typically comprise margin-parallel minor faults and fractures, as well as anastomosing minor faults. These minor faults typically comprise protobreccia, multiple mm-spaced margin parallel fractures, and may contain discontinuous mm-cm scale lenses of fault gouge (Figure 8e).

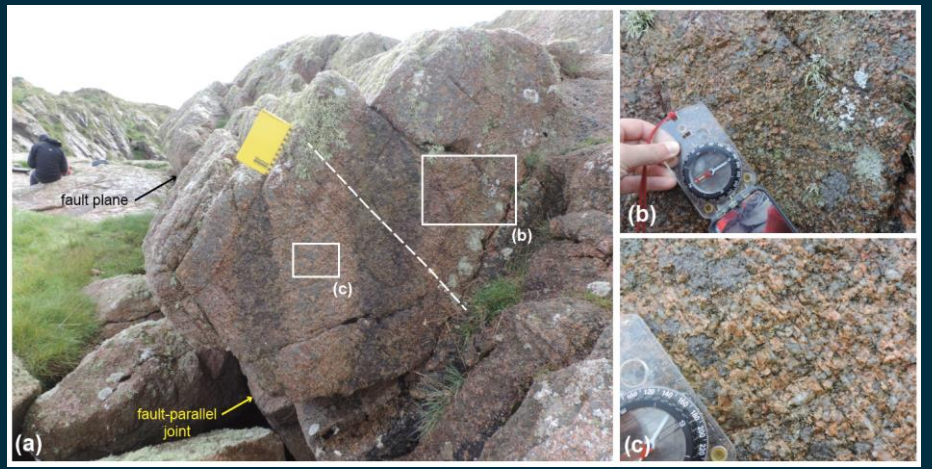

Figure 9. High fracture density adjacent to the main fault plane in the Boddam Fault Zone. BGS images P1080299, P1080300, P1080301 © UKRI 2024.

Boddam Fault

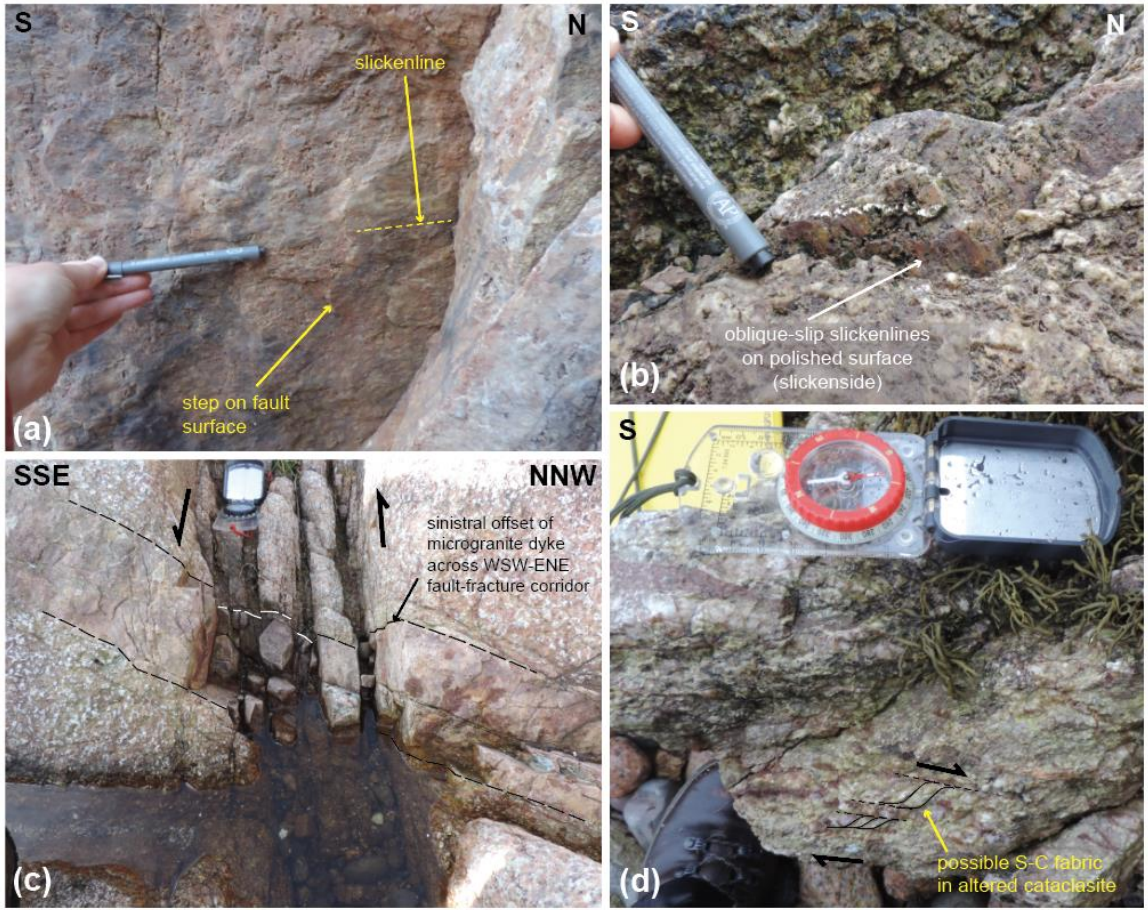

SLIP-SENSE INDICATORS

Fault surfaces within the Peterhead Granite are typically smooth and occasionally polished (slickensides). Shear sense has been interpreted from slickenlines, slickenfibres, and steps (which form perpendicular to slickenlines; Figure 10a-b), offset of microgranite dykes across faults and fault-fracture zones (Figure 10c), and S-C fabrics within cataclasite (Figure 10d).

Figure 10. Examples of shear-sense indicators. (a) slickenlines and steps at Bohham Lighthouse. (b) Slickenside and slickenlines at Boddam Lighthouse. (c) sinistral displacement across a WSW-ENE fault-fracture zone, recorded by offset microgranite dyke at Boddam Castle. (d) potential S-C fabric in cataclasite at Boddam Lighthouse. BGS images P1080216, P1080436, P1080359, P1080155

Boddam Castle

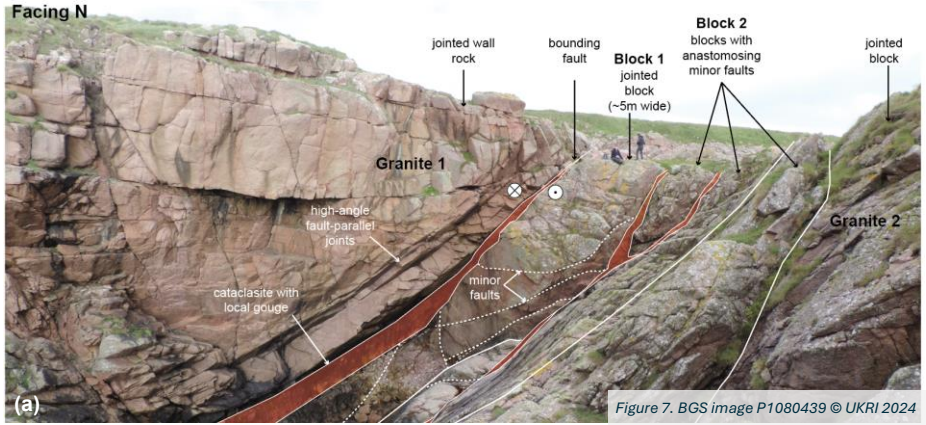

Figure 7. BGS image P1080439 © UKRI 2024

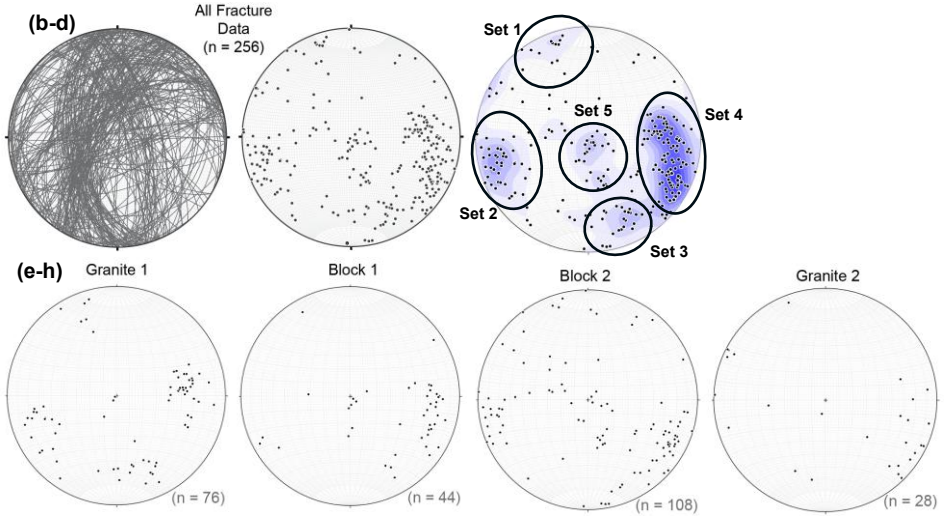

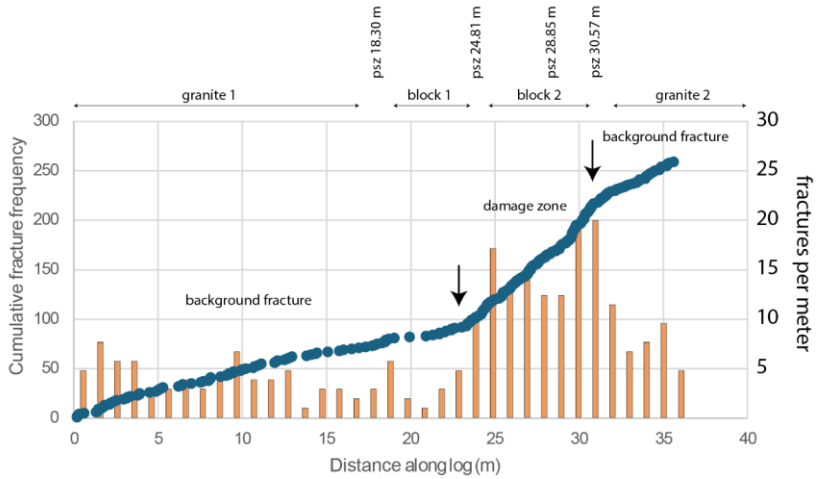

Figure 12. (Above) Cumulative fracture frequency (left y-axis) and fracture per meter (right y-axis) through the scanline transect. (x-axis) shows distance along the scanline intersecting Granite 1, blocks 1-2 and Granite 2. Granites 1-2 are considered background fracture frequency (number of fractures/m). Data collected and plotted by Mike Schiltz (TownRock Energy).

Figure 11. (Left) Lower hemisphere equal area stereonets of fracture data from Boddam Fault. (a-b) All data split by fracture sets in west block (granite 1), first fault block (block 1), second fault block (block 2), and east block (granite 2) for planes and pole-to-planes, and (c) contoured poles to planes to highlight fracture sets. (e-h) Stereonets showing fracture sets within each domain. Produced from data collected by Mike Schiltz (TownRock Energy).

FRACTURE CHARACTERISATION

A 1-D fracture scanline was conducted across part of the Boddam Fault to characterize fracture variability across the fault zone, due to time constraints only fractures with length ≥1 m were recorded. The site was divided into 4 domains: Granite 1 and 2 which bound the main Boddam Fault Zone, and Fault Blocks 1 and 2 within the fault zone, which are fault-bound lensoids of Granite.

The fracture data shows 5 fracture sets (Figure 11). The relative dominance of each fracture set changes between the domains, Granite 1 and Block 2 contain all fracture sets while Block 1 and Granite 2 are dominated by sets 4 and 5. The fracture frequency (number of fractures per meter; Sanderson and Nixon, 2015) is highest in blocks 1 and 2, shown by the sharp step in the cumulative frequency curve (Figure 12). The curve flattens off into the eastern bounding block (Granite 2) indicating a reduction in fracture frequency.

Boddam Lighthouse

At Boddam Lighthouse the fault zone occurs within a NNE-SSW trending inlet between the mainland and the islet hosting Boddam Lighthouse. Due to this, the majority of the inferred fault zone is eroded.

The fault zone follows the contact between a porphyritic microgranite intrusion (below Boddam Lighthouse) and the coarse granite of the Peterhead Pluton.

The following slides show the detailed structure of the fault zone in this location.

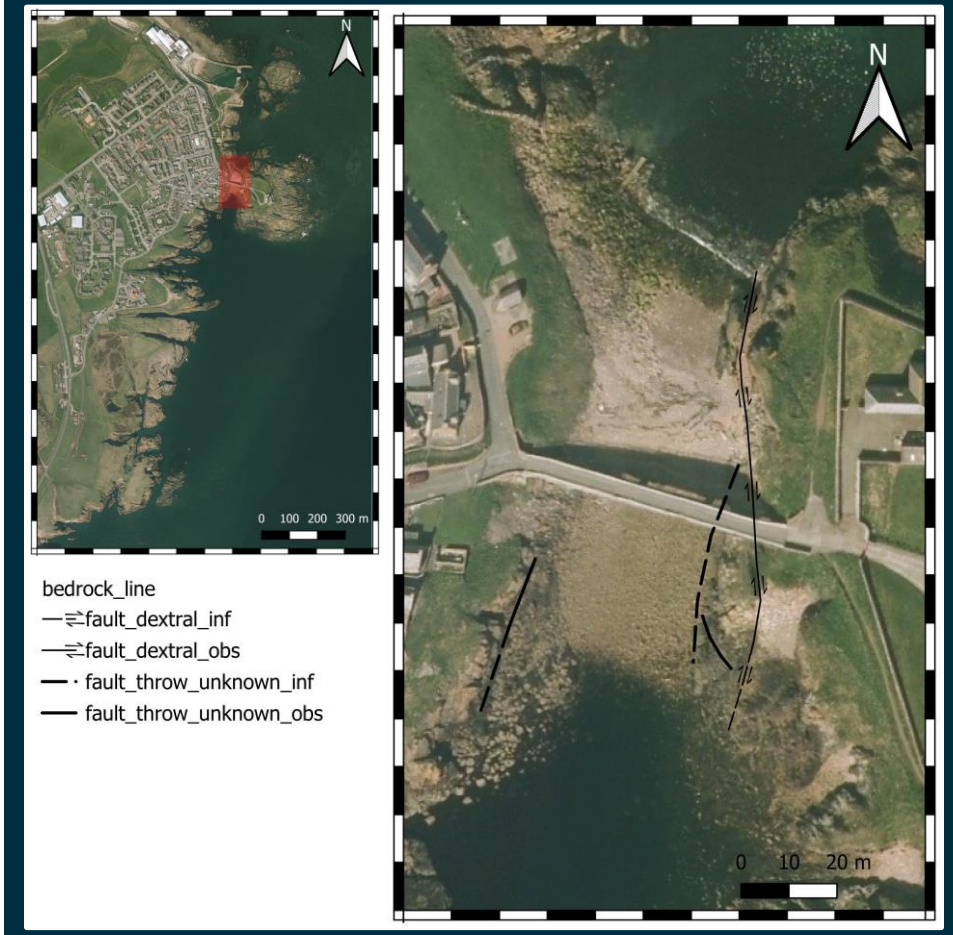

Figure 13. Map of Boddam Lighthouse Fault Zone with mapped structures, red square in the inset map shows the location of Boddam Lighthouse field area.

Boddam Lighthouse

FAULT ZONE ARCHITECTURE & FAULT ROCK

The fault core preserved in this area is quartz and haematite cemented and can be divided into multiple zones with lensoid geometries. The zones are listed from East to West (1-9) and shown in Figure 14:

1) Fractured porphyritic microgranite. Microgranite is finely crystalline (<1mm), pink-orange colour, with ~1 mm quartz phenocrysts. (Figure 14c, e)
2) Porphyritic microgranite, with increasing fracture density and lensoidal fracture geometries (Figure 14d). Fault-parallel quartz veins (~1-10 mm thick) become present towards the fault.
3) Aphanitic purple microgranite (inferred to be the chilled margin of the microgranite intrusion), with a high density of randomly oriented quartz veins, typically 1-2 mm thick (Figure 14f).
4) Quartz-Vein-Breccia with angular clasts of purple aphanitic microgranite (Figure 14g). Locally the breccia is chaotic and matrix-supported.
5) Quartz cut by red haematite veins, highly fractured and faulted. Cataclasite is altered to a green colour (Figure 14h).
6) Breccia with angular clasts of purple aphanitic microgranite with quartz-cemented matrix (Figure 14i).
7) Coarse granite breccia with cm-size lensoidal clasts of coarse granite (quartz and plagioclase crystals ~2-5 mm). The matrix is fine grained and haematite cemented (Figure 14j).
8) Coarse granite with quartz veins that trend NNW-SSE to N-S (Figure 14k).
9) Haematite-Quartz Breccia with clasts of coarse granite in a very fine grained, locally vuggy, quartz and haematite cemented matrix (Figure 14l).

Clast composition was consistent within individual fault lensoids, suggesting no mixing of adjacent wall rock material occurred during faulting, (except perhaps in the lensoid-bounding cataclasities).

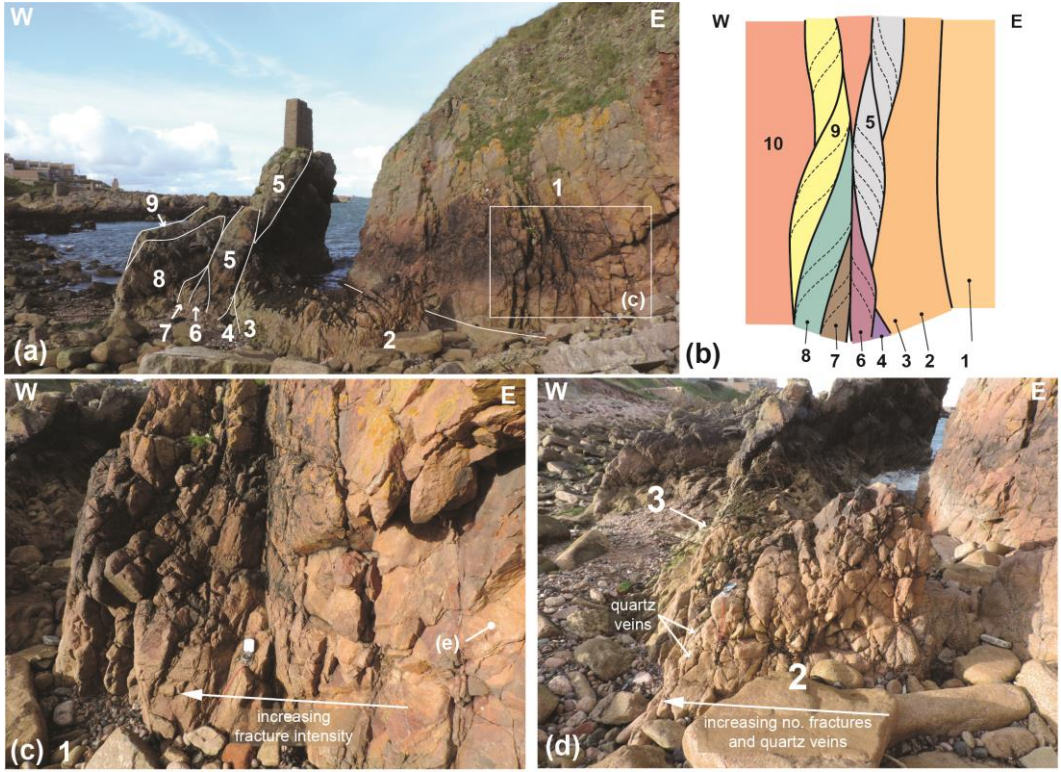

Figure 14. Boddam Lighthouse Fault Zone. (a) overview photograph; (b) schematic interpretation of the fault zone (British Geological Survey © UKRI 2026). (c) Zone 1, (d) Zone 2, see text for descriptions. BGS images P1080428, P1080440, P1080441 © UKRI 2024.

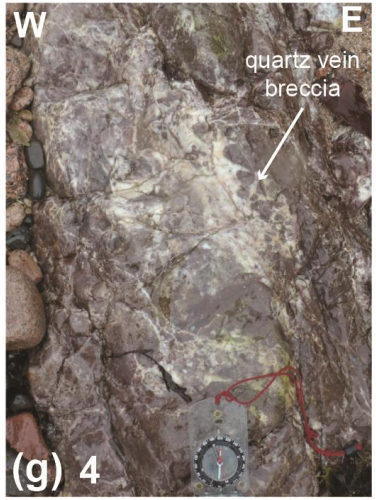

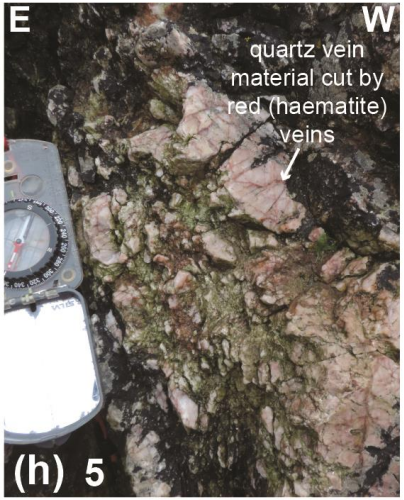

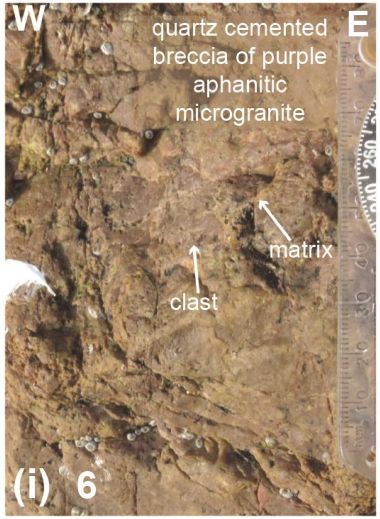

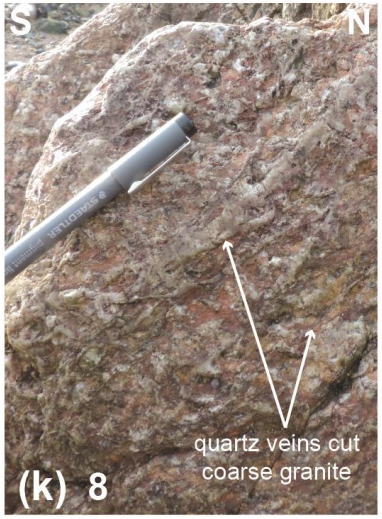

Figure 14 continued. See text for details.
BGS images P1080428, P1080439 , P1080443, P1080159, P1080419 , P1080454 , P1080459 , P1080462, P1080413

Boddam Lighthouse

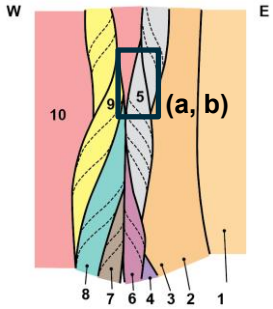

FAULT ROCK

Surfaces between lensoids are preferentially weathered and eroded (Figure 15). They contain up to c.5 cm width of cataclasite, which is locally foliated with foliation planes approximately parallel to the lensoid surface. Centimetre-width lenses of heamatite-cemented gouge also occur within the cataclasite (Figure 15b).

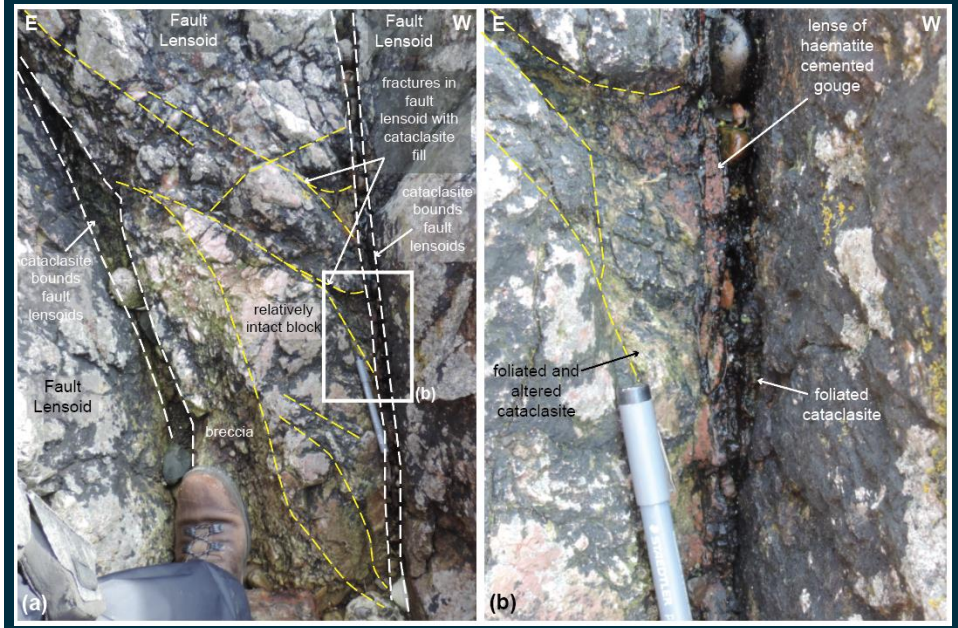

Figure 15. Fault-bound fractured lensoids within the Boddam Lighthouse Fault Zone. BGS images P1080425, P1080424 © UKRI 2024.

Boddam Lighthouse

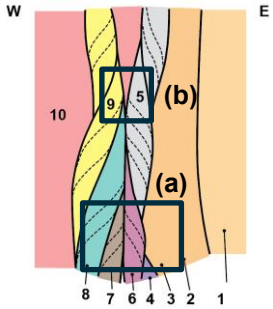

LENSOID STRUCTURE

Lensoids within the fault core at Boddam Lighthouse are m-scale structures with approximate minimum length and heights of 3 m and width of ~1 m, up to lengths of ~50 m and widths of ~15 m (Figure 16a-b).

Intra-lensoid fractures appear to be related to the lensoid attitude on either side of the main fault plane. This creates a series of different fracture orientations within the fault core (Figure 16 a-c).

The lensoids are formed of healed breccias. Fractures within the lensoids cross-cut the healed breccias (Figure 16d), indicating at least two stages of brittle deformation, (1) brecciation and cataclasis of the host lithology, followed by healing of the cataclasite matrix; (2) re-fracturing of the healed breccia.

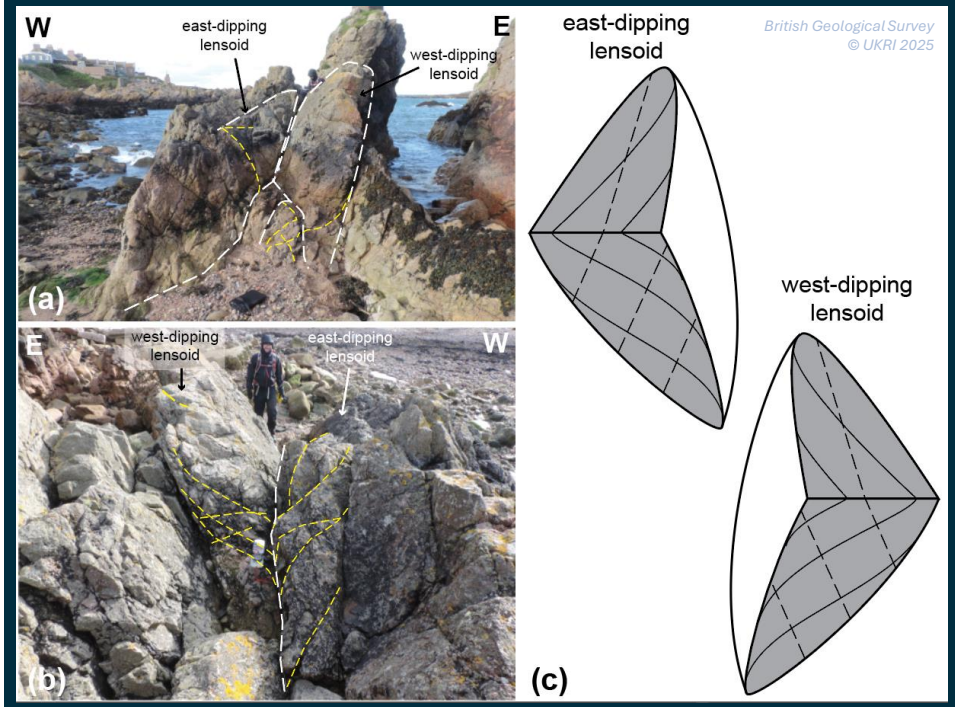

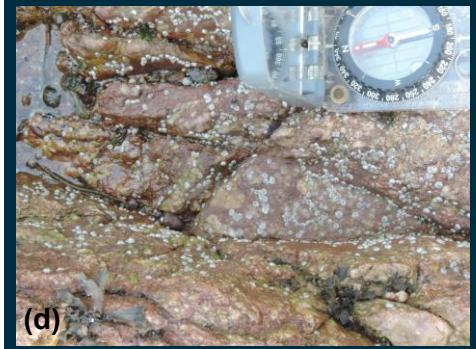

Figure 16. Fault-bound fractured lensoids within the Boddam Lighthouse Fault Zone. (a) Overview of fault-bound lensoid geometries. (b) fracture patterns within the lensoids (yellow dashed lines) . (c) schematic diagram of the relationship between lensoid geometry and internal fracture patterns. (d) fractured healed breccia. BGS images P1080427, P1080416, P1080457 © UKRI 2024.

Boddam Lighthouse

FRACTURE INTENSITY

Fracture intensity in the microgranite increases towards the fault plane. Fracture spacing within ~5 cm of the fault surface is extremely closely spaced with ~fault-parallel mm to cm spacing. At distances >5 cm from the fault fractures are very close to closely spaced and form two approximately orthogonal sets (oriented NE-SW and NNW-SSE). These joint sets have haematite-stained surfaces.

Fracture intensity and fracture orientation vary within the fault-bound lensoids (as shown on Slide 16).

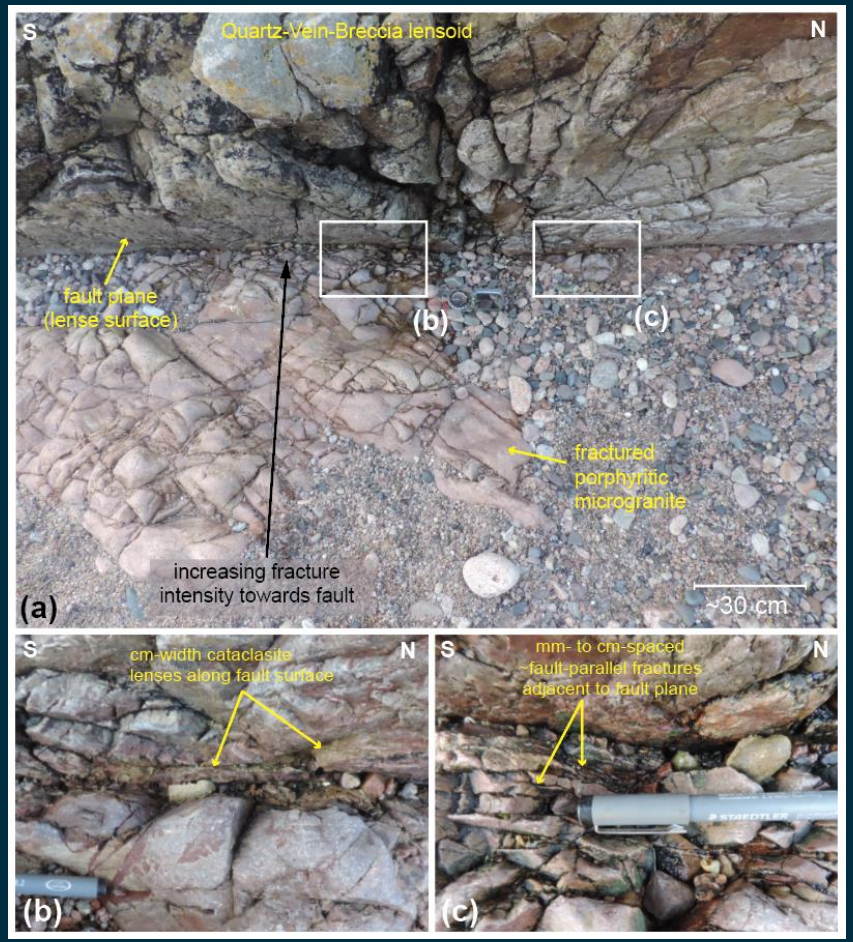

Figure 17. Boddam Lighthouse major fault pane, photos show increasing fracture spacing towards the fault plane (a), and zones of cataclasite along the fault surface. BGS images P1080208, P1080212, P1080210 © UKRI 2024.

Conceptual Model

The variety of faults observed at Boddam Castle are interpreted to represent a relay zone between two possibly underlapping dextral bounding faults (Figure 18):

- NNE-SSW orientated faults bound an area of high fracture intensity. These bounding faults are interpreted to show a dextral shear sense.
- The bounding fault is associated with a fault core comprised of an anastomosing network of principal slip surfaces that bound lenses of relatively intact rock
- ENE-WSW sinistral faults and NW-SE dextral faults are interpreted to represent R’ and P-shears within a Reidel Fault system. These faults appear to be constrained by the western bounding fault, and are interpreted as faults that accommodated strain transfer within a relay zone.
- N-S reverse faults are miss-matched relative to the dextral relay strain ellipsoid and may represent reactivation of earlier structures (e.g. joints within the granite) or a later phase of deformation.

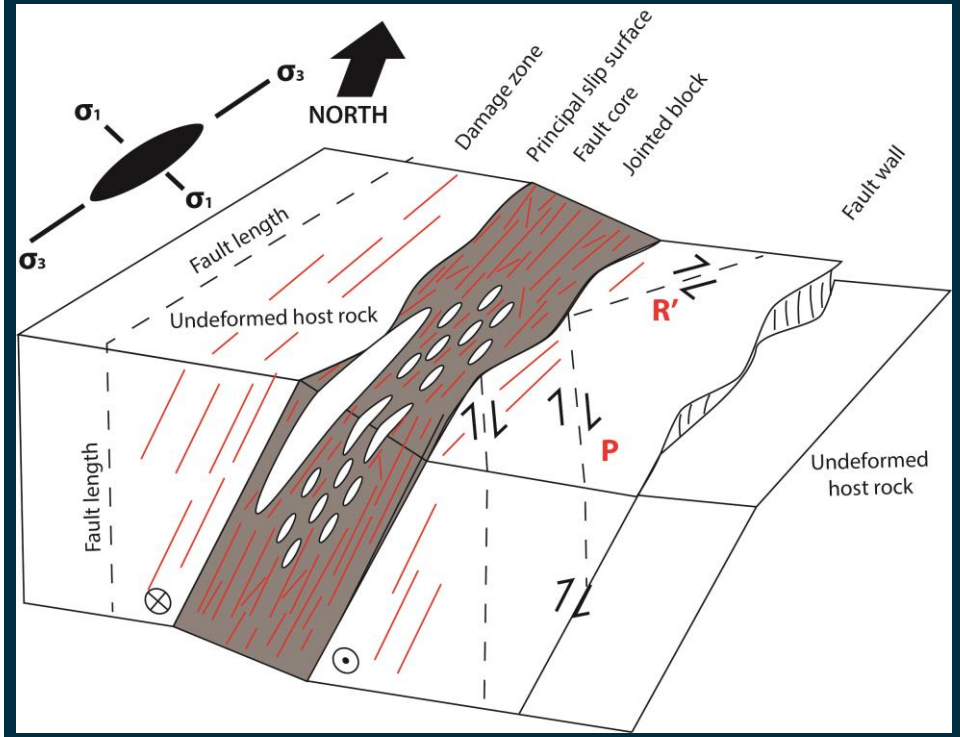

Figure 18. Conceptual block diagram to show the relationships between key features observed at the Boddam Castle Fault Zone. British Geological Survey © UKRI 2026.

Fluid flow and geothermal potential

Fault zone architecture and fault rock type are primary controls on fluid flow in upper-crustal, brittle fault zones within tight crystalline rock. Caine et al. (1996) use a qualitative model to define and estimate the relative permeability of a fault zone. They compare the percentage of the total fault zone width composed of fault core materials (e.g., anastomosing slip surfaces, clay-rich gouge, cataclasite, and fault breccias) to the percentage of subsidiary damage zone structures (e.g., kinematically related fracture sets, small faults, and veins). Additional consideration may be placed on the fault rock type, fault core material (particularly phyllosilicate gouges) creates barriers to fluid flow, while open damage zone structures and un-healed cataclasites and breccias can be fluid conduits (Caine et al., 1996; Faulkner et al. 2010 and references therein). Permeability and fluid transmissivity may therefore vary across a fault zone.

The Boddam Fault relay zone at Boddam Castle predominantly comprises proto-breccia and cataclasitie filled faults, with local gouges along the principal slip planes. Following the model of Caine et al. (1996) we suggest the Boddam Fault relay zone is a Distributed Conduit, considering a high ratio (>50%) of damage zone to fault core and low clay-fault gouge content (Figure 19). The relay zone is inferred to facilitate fault dip- and strike-parallel fluid flow through the zone, dip-orthogonal flow may be locally inhibited by gouge-filled bounding faults and locally enhanced by preferential flow along the Reidel fault-fracture corridors (Figure 19). Certain caution must be placed on estimated bulk fault zone permeability considering spatial and vertical heterogeneity on fault rock type, architecture, and fracture node connections (Faulkner et al. 2010). Many of the fractures observed at surface were open. This may result from weathering and removal of weaker or dissolvable fracture fills (such as clays or carbonate), meaning the fracture network at depth may contain a higher percentage of permeability-reducing material relative to the surface exposure. Despite this, the Boddam Fault relay zone is considered a good analogue for fault other faults in granite. Fault relay zones at depth analogous to the Boddam Fault relay zone, therefore, could be a potential geothermal target considering its distributed fracture networks and narrow fault core width.

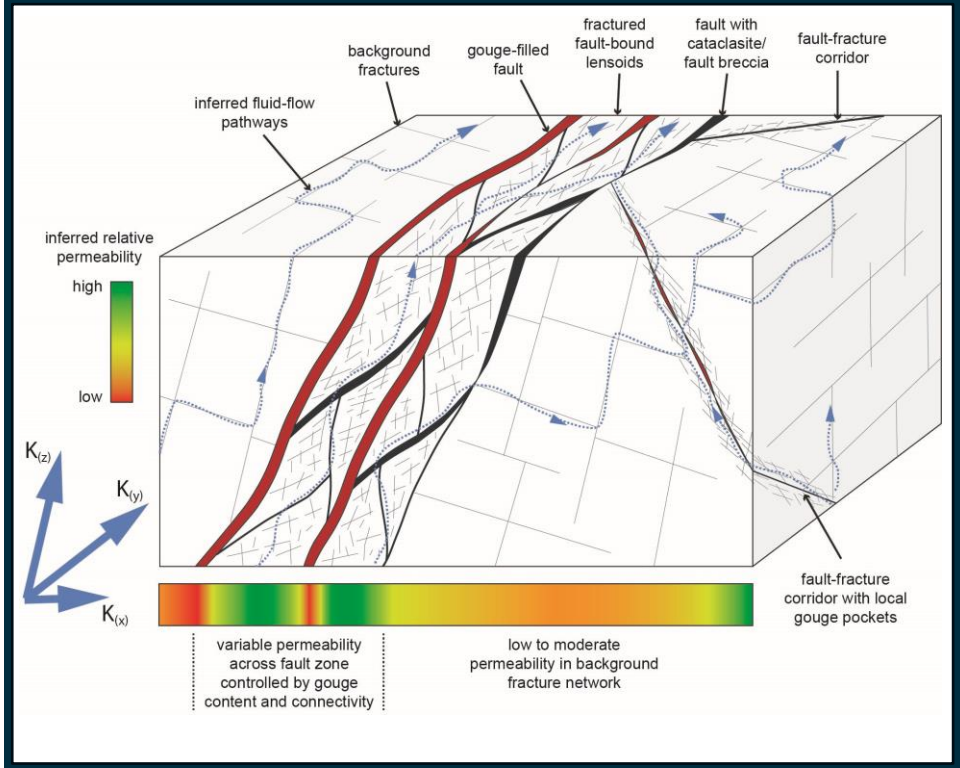

Figure 19. Conceptual block diagram to show inferred fluid flow pathways through the Boddam Fault Zone. Permeability and transmissivity is inferred to be higher parallel to dip and strike of the fault core and along Riedel Shears. Local flow barriers occur at gouge-filled faults. The background fracture network may allow additional vertical and lateral flow connectivity between the fault core and associated fault-fracture corridors. British Geological Survey © UKRI 2026.

Regional context

The Great Glen Fault and Walls Boundary Fault initiated during the late Caledonian orogeny (c. 420-400 Ma) as major sinistral faults.

The onset of the Variscan orogeny to the south of Britain and collision between Siberia and Fennoscandia in the Ural Orogeny to the east of Britain formed the supercontinent of Pangea, creating far field affects throughout the present-day North Atlantic region (Coward et al., 1989). In Southern Scotland, basin shortening and inversion is observed across the Midland Valley during Late Westphalian times. Here, many of the basin margin faults were reactivated with a reverse sense of displacement (Stone et al., 2012).

Further north, N-S dextral orientated features are observed on reactivated Caleodnian features such as the Walls Boundary Fault on Shetland (Armitage et al 2021;2024; Watts et al. 2007), and with inversion of Early Carboniferous normal faults across Norway and North Coast Transfer Zone (Coward et al., 1989; Roberts et al., 1999; Wilks and Cuthbert, 1994; Hartz et al., 1997), offering a stress regime with an E-W oriented σ_1 and N-S oriented σ_3.

The Boddam fault appears to fit an overall dextral fault system, suggesting it fits with a regional stress field of E-W oriented σ_1 and N-S oriented σ_3. It is unclear from the field observations whether the Boddam fault was initiated as a Caledonian structure and reactivated in a dextral setting, or whether the fault initiated in the Carboniferous as a primary dextral structure.

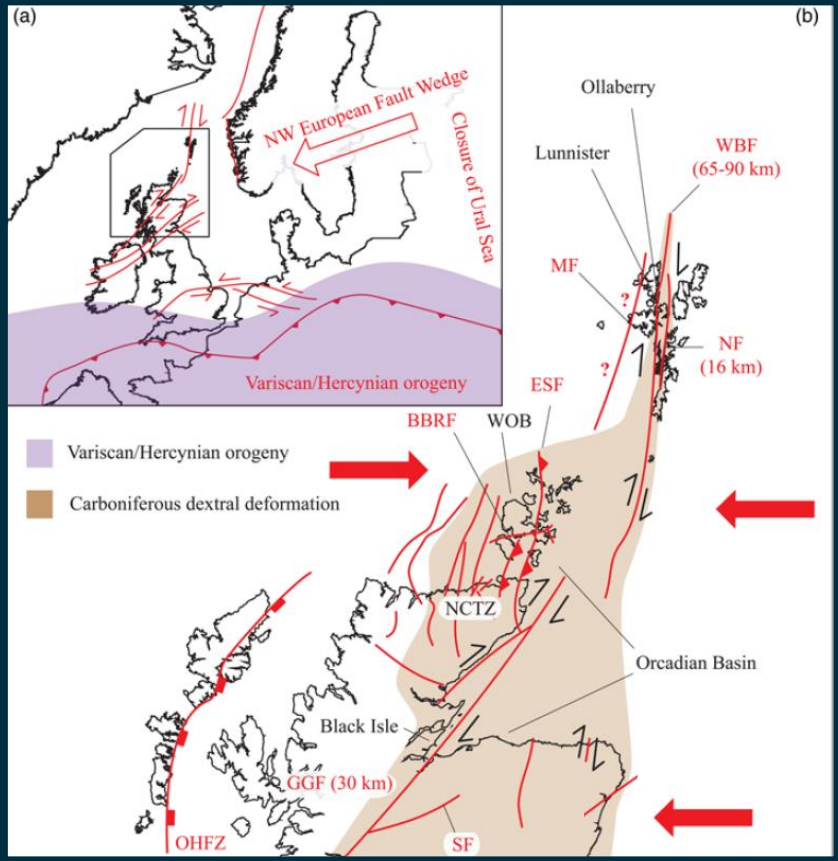

Figure 20. Regional tectonic setting for Late Carboniferous dextral reactivation on Caledonian and N-S orientated structures across Scotland (modified from Armitage et al. 2021, under the CC BY 4.0 licence).

Glossary (Gillespie et al., 2011)

Term	Definition
bedding	layering that formed during depositional processes and is sometimes preserved in metamorphic rocks, particularly in areas of low strain. Individual layers are typical made-up of contrasting grain sizes.
cataclasis	rock deformation achieved through the formation of fractures and rotation of constituent crystals, grains, or aggregates without chemical reconstitution
cataclasite	fault-rock that is cohesive with a poorly developed or absent schistosity, or which is incohesive, characterised by generally angular porphyroclasts and lithic fragments in a finer-grained matrix of similar composition; generally no preferred orientation of grains or individual fragments is present as a result of the deformation, but fractures may have a preferred orientation; a foliation is not generated unless the fragments are drawn out or new minerals grow during the deformation; plastic deformation may be present but is always subordinate to some combination of fracturing, rotation, and frictional sliding of particles; cf. fault-breccia, fault-gouge, protobreccia, protocataclasite, mesocataclasite, and ultracataclasite
cataclastic	texture produced by cataclasis, characterised by fractures, rotation of constituent crystals, grains, or aggregates
damage zone	a zone of elevated fracture frequency around a fault
discontinuity	a feature marking a change in the continuity of a material at the scale of interest or observation; also, the generic term for all such features
fault	a fracture formed by, or incorporating, shearing displacement, along which there is discernible displacement parallel to the bounding surfaces at the scale of observation
fault-breccia	cataclasite, of which more than 30% consists of visible wallrock clasts, the remainder being dominated by very fine authigenic minerals (e.g. clay and Fe/Mn oxide/oxyhydroxide); cf. fault-gouge

Term	Definition
fracture	a deformation-break characterised by a discontinuous change in strength and/or stiffness, such that there is a stepwise change in the displacement distribution across it; the volume of deformed material associated with fractures (not including filling) typically has negligible thickness at the scale of observation (hence their surfaces are perceived to be sharply defined); such features typically consist of two opposing surfaces in contact or close proximity
joint	a fracture formed by opening displacement, synonymous with crack
mesocataclasite	cataclasite in which the matrix forms more than 50% and less than 90% of the rock volume
protobreccia	cataclasite in which the matrix forms less than 10% of the rock volume
protocataclasite	cataclasite in which the matrix forms between 10 and 50% of the rock volume
relay zone	a zone in between two related fault segments, where displacement is transferred (‘relayed’) from one fault segment to another; typically marked by a series of minor faults oblique to the main fault segments
slickenline	lineation on a slickenside, defined by grooves, ridges or striations, generally parallel to the direction of the slip vector
slickenside	polished fault surface (with or without lineations)
splay	a fault developed as an offshoot from another fault
ultracataclasite	cataclasite in which the matrix forms more than 90% of the rock volume

References

Archibald, D.B., Murphy, J.B., Fowler, M., Strachan, R.A. and Hildebrand, R.S., 2022. Testing petrogenetic models for contemporaneous mafic and felsic to intermediate magmatism within the “Newer Granite” suite of the Scottish and Irish Caledonides. https://doi.org/10.1130/2021.2554(15)

Armitage, T.B., Watts, L.M., Holdsworth, R.E. and Strachan, R.A., 2021. Late Carboniferous dextral transpressional reactivation of the crustal-scale Walls Boundary Fault, Shetland: the role of pre-existing structures and lithological heterogeneities. *Journal of the Geological Society*, *178*(1), pp.jgs2020-078. https://doi.org/10.1144/jgs2020-078

Armitage, T.B., Holdsworth, R.E., Strachan, R.A., Dempsey, E.D., Walker, R.J., Alvarez-Ruiz, D.T. and Lloyd, G.E., 2024. Overprinting orogenic events, ductile extrusion and strain partitioning during Caledonian transpression, NW Mainland Shetland. *Journal of Structural Geology*, *180*, p.105088. https://doi.org/10.1016/j.jsg.2024.105088

Atherton, M.P. and Ghani, A.A., 2002. Slab breakoff: a model for Caledonian, Late Granite syn-collisional magmatism in the orthotectonic (metamorphic) zone of Scotland and Donegal, Ireland. *Lithos*, *62*(3-4), pp.65-85. https://doi.org/10.1016/S0024-4937(02)00111-1

Caine, J. S., Evans, J. P., & Forster, C. B. (1996). Fault zone architecture and permeability structure. *Geology*, 24(11), 1025. https://doi.org/10.1130/0091-7613(1996)024<1025:FZAAPS>2.3.CO;2

Coward, M.P., Enfield, M.A. and Fischer, M.W., 1989. Devonian basins of Northern Scotland: extension and inversion related to Late Caledonian—Variscan tectonics. *Geological Society, London, Special Publications*, *44*(1), pp.275-308. https://doi.org/10.1144/GSL.SP.1989.044.01.16

Gillespie, M.R., Barnes, R.P. and Milodowski, A.E., 2011. British Geological Survey scheme for classifying discontinuities and fillings. British Geological Survey.

Faulkner, D.R., Jackson, C.A.L., Lunn, R.J., Schlische, R.W., Shipton, Z.K., Wibberley, C.A.J. and Withjack, M.O., 2010. A review of recent developments concerning the structure, mechanics and fluid flow properties of fault zones. *Journal of Structural Geology*, *32*(11), pp.1557-1575. https://doi.org/10.1016/j.jsg.2010.06.009

Hartz, E.H. and Andresen, A., 1997. From collision to collapse: Complex strain permutations in the hinterland of the Scandinavian Caledonides. *Journal of Geophysical Research: Solid Earth*, *102*(B11), pp.24697-24711. https://doi.org/10.1029/97JB02275

Haughton, P.D.W. and Halliday, A.N., 1991. Significance of a late Caledonian igneous complex revealed by clasts in Lower Old Red Sandstone conglomerates, central Scotland. *Geological Society of America Bulletin*, *103*(11), pp.1476-1492. https://doi.org/10.1130/0016-7606(1991)103%3C1476:SOALCI%3E2.3.CO;2

Oliver, G.J., Wilde, S.A. and Wan, Y., 2008. Geochronology and geodynamics of Scottish granitoids from the late Neoproterozoic break-up of Rodinia to Palaeozoic collision. *Journal of the Geological Society*, *165*(3), pp.661-674. https://doi.org/10.1144/0016-76492007-105

Lambert, R.S.J. and McKerrow, W.S., 1976. The Grampian Orogeny. *Scottish Journal of Geology*, *12*(4), pp.271-292. https://doi.org/10.1144/sjg12040271

Roberts, D.G., Thompson, M., Mitchener, B., Hossack, J., Carmichael, S. and Bjørnseth, H.M., 1999. Palaeozoic to Tertiary rift and basin dynamics: mid-Norway to the Bay of Biscay–a new context for hydrocarbon prospectivity in the deep water frontier. In Geological Society, London, Petroleum Geology Conference Series (Vol. 5, No. 1, pp. 7-40). *The Geological Society of London*. https://doi.org/10.1144/0050007

Sanderson, D.J. and Nixon, C.W., 2015. The use of topology in fracture network characterization. Journal of Structural Geology, 72, pp.55-66. http://dx.doi.org/10.1016/j.jsg.2015.01.005

Stone P., McMillan A. A., Floyd J. D., Barnes R. P., and Phillips E. R. 2012. British Regional Geology: South of Scotland (4th edn). *British Geological Survey, Nottingham*. 247 pp. https://doi.org/10.1144/sjg2014-003

Watts, L.M., Holdsworth, R.E., Sleight, J.A., Strachan, R.A. and Smith, S.A.F., 2007. The movement history and fault rock evolution of a reactivated crustal-scale strike-slip fault: the Walls Boundary Fault Zone, Shetland. *Journal of the Geological Society*, 164(5), pp.1037-1058. https://doi.org/10.1144/0016-76492006-156

Wilks, W.J. and Cuthbert, S.J., 1994. The evolution of the Hornelen Basin detachment system, western Norway: implications for the style of late orogenic extension in the southern Scandinavian Caledonides. *Tectonophysics*, 238(1-4), pp.1-30. https://doi.org/10.1016/0040-1951(94)90047-7